PROCEEDINGS OF SCIENCE

Lepton Universality tests using semileptonic b-hadron decays

Resmi P. K.[†,*]

Aix Marseille Univ, CNRS/IN2P3, CPPM
163 avenue de Luminy, Case 902 13288 Marseille cedex 09, France

E-mail: resmi.pk@cern.ch

The Standard Model is lepton flavour universal *i.e.* the couplings between electroweak gauge bosons and the different lepton families are universal. However, recent measurements have shown deviations from this behavior, which could potentially be due to contribution from new physics beyond the Standard Model. The lepton flavour universality tests done at the LHCb experiment using tree-level b-hadron decays are presented.

41st International Conference on High Energy physics - ICHEP2022
6-13 July, 2022
Bologna, Italy

[†]on behalf of LHCb Collaboration.
[*]Speaker

PoS(ICHEP2022)739

1. Introduction

In the Standard Model (SM), electroweak couplings to all charged leptons are universal and any difference between e, μ and τ is driven by the difference in their mass. The lepton flavour universality (LFU) is tested using ratios of branching fractions of decays involving different leptons [1]. In $b \to c\ell\nu_\ell$ transitions, the ratio $R(X_c) = \frac{\mathcal{B}(X_b \to X_c \tau^+ \nu_\tau)}{\mathcal{B}(X_b \to X_c \ell \nu_\ell)}$ is measured, where X_b (X_c) is a hadron containing b (c) quark and $\ell = e, \mu$. These ratios are sensitive to possible enhanced couplings to the third generation of quarks predicted by some models involving physics beyond SM [2]. The uncertainties related to form factors mostly cancel in these ratios. The $R(X_c)$ ratio measurements performed at LHCb are presented here.

2. $R(X_c)$ measurements

The ratios $R(\Lambda_c)$, $R(D^*)$ and $R(J/\psi)$ are measured at LHCb using the Run 1 data sample collected during 2011 and 2012, corresponding to an integrated luminosity of 3 fb^{-1}. In general, two types of τ decays are identified: muonic, $\tau^- \to \mu^- \nu_\mu \nu_\tau$ and three-prong hadronic, $\tau^- \to \pi^+\pi^-\pi^-(\pi^0)\nu_\tau$. The $R(D^*)$ masurements explore both the decay modes. The $R(J/\psi)$ and $R(\Lambda_c)$ measurements are performed with muonic and hadronic τ decays, respectively. Neutrinos are not reconstructed for any of the decays and specific approximations are used to reconstruct the b-hadron candidates.

2.1 Measurements with hadroninc τ decays

The latest $R(X_c)$ ratio measurement from LHCb involves $\Lambda_b^0 \to \Lambda_c^+ \tau^- \bar{\nu}_\tau$ decays [3] in which the τ is reconstructed from three-prong hadronic decays to pions. This is the first LFU test done in a baryonic $b \to c\ell\nu_\ell$ decay. This measurement provides complementary constraints on LFU due to the half-integer spin of the initial state. The branching fraction of the signal decay is normalised with that of $\Lambda_b^0 \to \Lambda_c^+ 3\pi^\pm$, which has the same visible final state. Their ratio, $\mathcal{K}(\Lambda_c)$ is then converted into $R(\Lambda_c)$ as $R(\Lambda_c) = \mathcal{K}(\Lambda_c) \frac{\mathcal{B}(\Lambda_b^0 \to \Lambda_c^+ 3\pi^\pm)}{\mathcal{B}(\Lambda_b^0 \to \Lambda_c^+ \mu^- \nu_\mu)}$.

The decays of the type $\Lambda_b \to \Lambda_c^+ \pi\pi\pi X$, where the three charged pions come directly from the Λ_b baryon, form the dominant backgrounds. They are also termed as "prompt" decays. These are suppressed by requiring that the $3\pi^\pm$ vertex is displaced from that of Λ_b by at least five times larger than the uncertainty on its position. The remaining major background contribution is from Λ_b decays to Λ_c^+ and another charm hadron, mainly D_s^-, which further decays into a final state having three charged pions. These are termed as "double charm" decays. They mimic the signal topology due to the non-negligible lifetime of the charm hadrons. These are reduced using a boosted decision tree (BDT) classifier which exploits the difference in decay dynamics of τ^- and D_s^-. These background events are further studied using simulated samples of $\Lambda_b \to \Lambda_c^+ D_s^- X$ decays that are validated using data control samples. The fractions of various such decays are estimated from a binned template fit to $\Lambda_c^+ 3\pi^\pm$ invariant mass, as shown in Fig. 1. These background fractions are used as constraints in the signal extraction fit.

The signal yield is extracted from a three-dimensional binned template fit to $q^2 = (p_{\Lambda_b} - p_{\Lambda_c})^2$, τ^- decay time, and the BDT output, where p is the momentum of the corresponding particle. The templates representing probability density functions for the signal and background components are

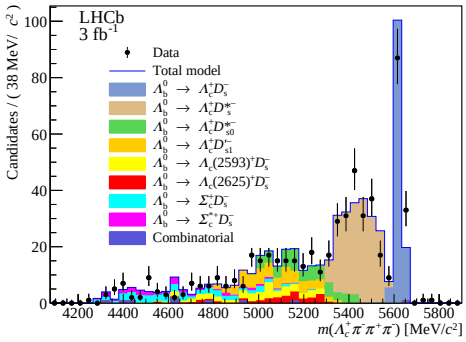

Figure 1: Distributions of the $\Lambda_c^+ 3\pi^\pm$ invariant mass for $\Lambda_b^0 \to \Lambda_c^+ D_s^+ X$ control sample.

extracted from control samples and simulations that are validated against data. The fit projections are shown in Fig. 2. There are 349 ± 40 signal decays and this is the first observation of $\Lambda_b^0 \to \Lambda_c^+ \tau^- \bar{\nu}_\tau$ with a significance of 6σ. The result $R(\Lambda_c) = 0.242 \pm 0.026(\text{stat}) \pm 0.040(\text{syst}) \pm 0.059(\text{ext})$ is lower than the SM predicted value [4] but in agreement within 1σ; where the last uncertainty is due to the external inputs. The dominant source of systematic uncertainty is from the knowledge of the double charm background template shapes.

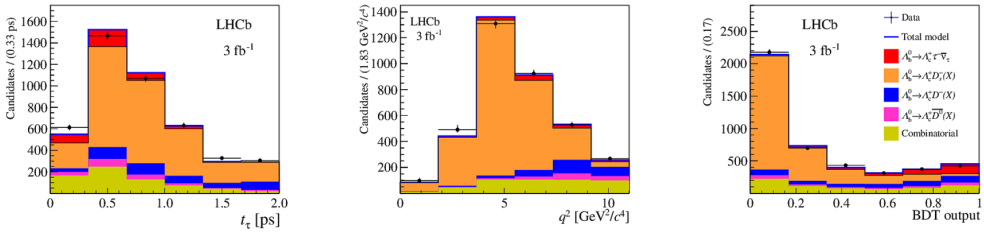

Figure 2: Distributions of τ decay time (left), q^2 (middle) and BDT output (right) of the signal data, overlaid with projections of the fit model with all normalization and shape parameters at their best-fit values for $\Lambda_b^0 \to \Lambda_c^+ \tau^- \bar{\nu}_\tau$ candidates.

A new interpretation of the $R(\Lambda_c)$ measurement is discussed in ref [5]. Instead of using the $\mathcal{B}(\Lambda_b^0 \to \Lambda_c^+ \mu^- \nu_\mu)$ from PDG as external input [6], it is suggested to use the SM prediction since the former might not incorporate potentially important corrections and correlations. This reduces the significance of the hint for a suppression of $R(\Lambda_c)$. The fraction of excited states in inclusive Λ_b decays is greater than that in B decays and hence more experimental and theoretical insights are needed in this front.

The hadronic τ decays are also utilised to measure $R(D^*)$ [7, 8] using $B^0 \to D^{*-} \tau^+ \nu_\tau$ decays with $B^0 \to D^{*-} 3\pi^\pm$, which has the same visible final state, as a normalisation mode.The parameters are measured as $R(D^*) = \mathcal{K}(D^*) \frac{\mathcal{B}(B^0 \to D^{*-} 3\pi^\pm)}{\mathcal{B}(B^0 \to D^{*-} \ell \nu_\ell)}$, where $\mathcal{K}(D^*) = \frac{\mathcal{B}(B^0 \to D^{*-} \tau^+ \nu_\tau)}{\mathcal{B}(B^0 \to D^{*-} 3\pi^\pm)}$ is measured and the other branching fractions are taken as external inputs [1, 6]. The τ decay vertex is reconstructed from the three charged pion daughter candidates. The dominant backgrounds include $B \to D^{*-} 3\pi^\pm X$ prompt decays and $B \to D^{*-}(D_s^+, D^+, D^0) X$ double-charm decays. The prompt

decays are suppressed by requiring that the $3\pi^{\pm}$ vertex is displaced with respect to that of the B. The double charm backgrounds are suppressed with the help of a BDT classifier.

A three-dimensional binned template fit is used to extract the signal yield, with the variables $q^2 = (p_{B^0} - p_{D^*})^2$, τ^+ decay time, and the output of BDT trained to discriminate τ from D_s^+. The fit projections are shown in Fig. 3. The result, $R(D^*) = 0.280 \pm 0.018(\text{stat}) \pm 0.026(\text{syst}) \pm 0.013(\text{ext})$, is 1σ above the expected value from SM. The dominant systematic uncertainty is due to the limited size of the simulation sample.

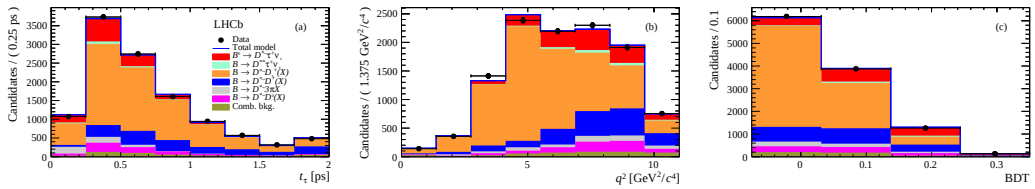

Figure 3: Distributions of τ decay time (left), q^2 (middle) and BDT output (right) of the signal data, overlaid with projections of the fit model with all normalization and shape parameters at their best-fit values for $B^0 \to D^{*-}\tau^+\nu_\tau$ candidates.

2.2 Measurements with muonic τ decays

The ratio $R(D^*) = \frac{\mathcal{B}(B\to D^*\tau\nu)}{\mathcal{B}(B\to D^*\mu\nu)}$ is measured with the muonic τ decays [9]. The B candidate reconstruction is carried out with the approximation that the z-component of the B momentum is the same as that of the $D^*\mu$ system. The visible final state in both the decay modes, in the numerator and denominator of $R(D^*)$, is the same. The τ and μ decay modes are separated via a three-dimensional binned template fit to the variables $q^2 = (p_B - p_{D^*})^2$, $m^2_{\text{miss}} = (p_B - p_{D^*} - p_\ell)^2$ and E^*_μ, energy of the muon in the B rest frame.

A BDT classifier is used to reject backgrounds with additional charged tracks. The final selected sample contains backgrounds of the types, $B \to D^{**}\mu\nu$, $B \to D^{**}\tau\nu$, $B_s \to D_s\mu\nu$, $B \to D^{*+}H_cX$, where H_c decays semileptonically, random final state combinations, and hadrons (π, K, p) misidentified as muons. The fit extracts the relative contributions of signal and normalization modes along with their form factors. The fit projections are shown in Fig. 4. The result obtained, $R(D^*) = 0.336 \pm 0.027(\text{stat}) \pm 0.030(\text{syst})$, is 2.1σ above the SM prediction. The dominant systematic uncertainty comes from the limited size of the simulation sample.

The ratio $R(J/\psi) = \frac{\mathcal{B}(B_c^+\to J/\psi\,\tau^+\nu_\tau)}{\mathcal{B}(B_c^+\to J/\psi\,\mu^+\nu_\mu)}$ is also measured using the muonic decays of τ [10]. Signal is extracted using a binned template fit to m^2_{miss}, B_c decay time and Z, where Z contains 8 bins in E^*_μ and q^2 (first 4 bins with $q^2 < 7.14$ GeV^2, the rest $q^2 > 7.14$ GeV^2). The fit results are given in Fig. 5. This is the first evidence of the $B_c^+ \to J/\psi\,\tau^+\nu_\tau$ decay mode. The $R(J/\psi)$ value obtained is $0.71 \pm 0.17(\text{stat}) \pm 0.18(\text{syst})$, which is 2σ above the predicted value from SM.

The measurements show deviations from the SM expectations. In particular, the combination of $R(D)$ and $R(D^*)$ measurements is more than 3σ away from the predictions in the SM [1]. Therefore it is important to improve the measurements with more data and devise strategies to reduce dominant systematic uncertainties. More $R(X_c)$ measurements are being performed at LHCb. Furthermore, new observables beyond the branching fraction ratios are being explored to study the nature of potential new physics.

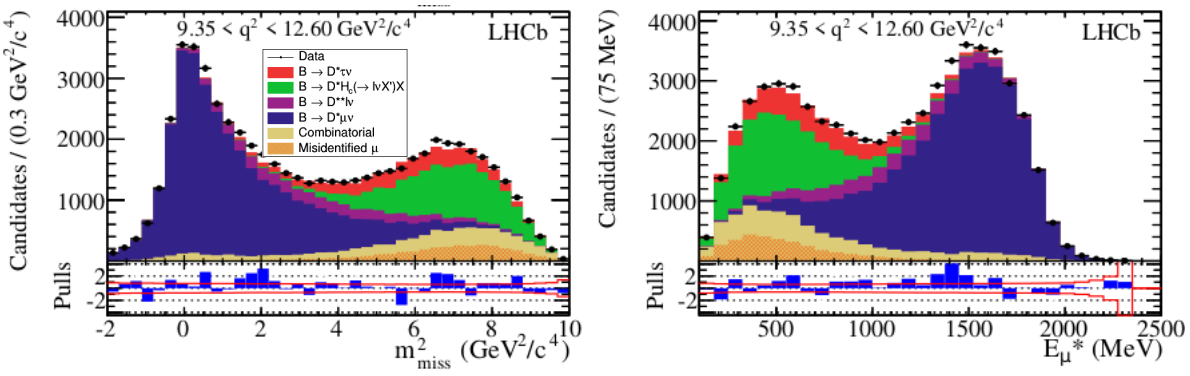

Figure 4: Distributions of m^2_{miss} (left) and $E^*_{\mu^+}$ (right) in the specified q^2 bins of the signal data, overlaid with projections of the fit model with all normalization and shape parameters at their best-fit values.

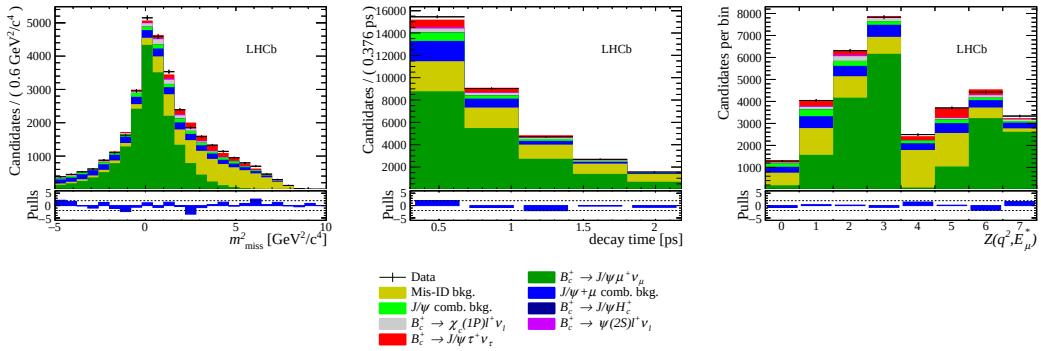

Figure 5: Distributions of m^2_{miss} (left), decay time (middle) and Z (right) of the signal data, overlaid with projections of the fit model with all normalization and shape parameters at their best-fit values.

3. Summary and prospects

There are several tensions with the SM predictions observed in the behaviour of leptons in semileptonic b-hadron decays. There are tensions up to 3σ found in measurements involving $b \to c\ell\nu_\ell$ decays. New measurements and observables are needed to understand the nature of these discrepancies and identify the possible sources of new physics, if any. The Run 3 data taking at LHCb will start very soon during which the LHCb detector is expected to collect data corresponding to an integrated luminosity of 25 fb^{-1}. The expected sensitivity of $R(X_c)$ measurements with future datasets from LHCb is illustrated in Fig. 6 [11, 12]. Also thanks to improved trigger and reconstruction techniques, this will allow more precise measurements to be made and many new observables to be explored, thus helping to further understand the nature of leptons within the SM and beyond.

References

[1] Y. Amhis *et al*. (Heavy Flavour Averaging Group), Eur. Phys. J. **C81** 226 (2021).

[2] A. Crivellin, J. Heeck, and P. Stoffer, Phys. Rev. Lett. **116**, 081801 (2016).

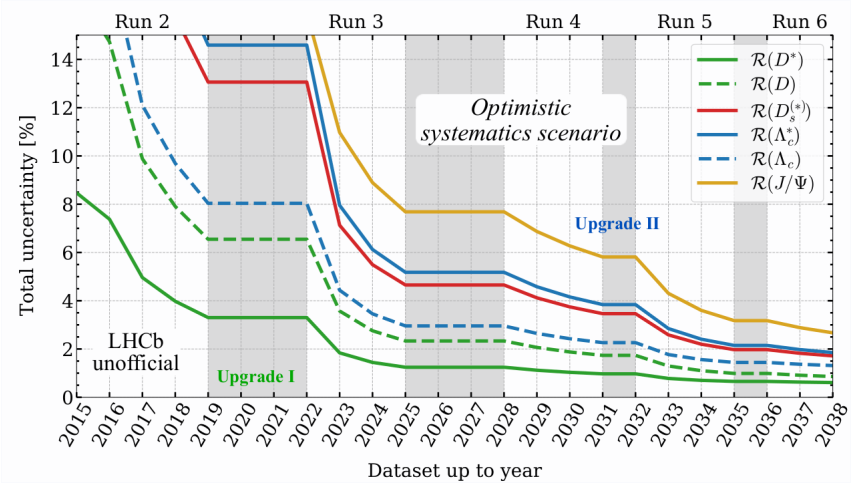

Figure 6: Projections for the expcted precision of $R(X_c)$ measurements at LHCb as a function of year in which the corresponding data sample is available [11, 12].

[3] R. Aaij *et al*. (LHCb Collaboration), Phys. Rev. Lett. **128**, 191803 (2022).

[4] F. U. Bernlochner, Z. Ligeti, D. J. Robinson and W. L. Sutcliffe, Phys. Rev. D. **99**, 055008 (2019).

[5] F. U. Bernlochner, Z. Ligeti, M. Papucci and D. J. Robinson, arXiv:2206.11282v1 [hep-ph].

[6] R. L. Workman et al. (Particle Data Group), Prog. Theor. Exp. Phys. **2022**, 083C01 (2022)

[7] R. Aaij *et al*. (LHCb Collaboration), Phys. Rev. Lett. **120**, 171802 (2018).

[8] R. Aaij *et al*. (LHCb Collaboration), Phys. Rev. D. **97**, 072013 (2018).

[9] R. Aaij *et al*. (LHCb Collaboration), Phys. Rev. Lett. **115**, 111803 (2015).

[10] R. Aaij *et al*. (LHCb Collaboration), Phys. Rev. Lett. **120**, 121801 (2018).

[11] F. U. Bernlochner, M. F. Sevilla, D. J. Robinson and G. Wormser arXiv:2101.08326v1 [hep-ex].

[12] R. Aaij *et al*. (LHCb Collaboration), arXiv:1808.08865v4 [hep-ex].